Numerical Simulation of Louisiana Shelf Circulation under Hurricane Katrina

Authors: Allahdadi, Mohammad Nabi, and Li, Chunyan

Source: Journal of Coastal Research, 34(1) : 67-80

Published By: Coastal Education and Research Foundation

URL: https://doi.org/10.2112/JCOASTRES-D-16-00129.1

Journal of Coastal Research	34	1	67–80	Coconut Creek, Florida	January 2018

Numerical Simulation of Louisiana Shelf Circulation under Hurricane Katrina

Mohammad Nabi Allahdadi* **and Chunyan Li**

Coastal Studies Institute
Department of Oceanography and Coastal Sciences
College of the Coast and Environment
Louisiana State University
Baton Rouge, LA 70803, U.S.A.

www.cerf-jcr.org

www.JCRonline.org

ABSTRACT

Allahdadi, M.N. and Li, C., 2018. Numerical simulation of Louisiana shelf circulation under Hurricane Katrina. *Journal of Coastal Research,* 34(1), 67–80. Coconut Creek (Florida), ISSN 0749-0208.

The response of currents on the Louisiana shelf to Hurricane Katrina was studied using the 3-D Finite Volume Community Ocean Model (FVCOM). The study area encompassed the Louisiana shelf covering both sides of the Mississippi River's Birdsfoot Delta. The model was forced by a wind field prepared by combining the Hurricane Research Division Wind Analysis System data for the hurricane with background winds outside of the hurricane's influence from National Centers for Environmental Prediction (NCEP)/North American Regional Reanalysis (NARR). Current and water-level data recorded at Wave-Current-Surge Information System (WAVCIS) stations over the inner shelf provided a unique opportunity to examine shelf hydrodynamics in response to Katrina. Model performance was evaluated by examining water-column stratification under different scenarios and using a range of parameters of the Mellor-Yamada level 2.5 turbulence closures for vertical eddy viscosity. This resulted in a set of appropriate closure parameters for the response of a shallow shelf to a hurricane. Simulated near-surface currents followed the overall pattern of hurricane wind structure over the outer shelf and to some extent over the inner shelf; however, currents over the shallow Louisiana shelf were affected by coastal geometry. Investigation of bottom currents showed a possible baroclinic response over both the inner and outer shelves. Over the Louisiana shelf, this was similar to the baroclinic response of stratified shallow waters for regions outside of the radius of maximum wind (R_{mw}), as identified in previous studies. A part of this baroclinic response can be explained by the horizontal baroclinic pressure gradient that resulted from the inhomogeneous hurricane-induced surface cooling.

ADDITIONAL INDEX WORDS: *Hydrodynamics, baroclinic, barotropic, stratification, FVCOM.*

INTRODUCTION

The energetics of hurricanes tremendously affects ocean/shelf water and produces large waves, storm surges, and enhanced current velocities. Waves generated by hurricanes can damage offshore structures (such as oil rigs) and coastal facilities (Cooper and Thompson, 1989a). Large hurricane storm surges are a serious threat to coastal areas and people's lives, especially in the vicinity of the hurricane's landfall (Chen, Wang, and Zhao, 2009). Hurricane-induced currents and waves may cause significant coastal erosion and redistribution of sediments, as well as significant sediment transport in coastal waters and on the continental shelf. Furthermore, strong horizontal velocity shear along with large waves can mix the water column and break down the stratification. This can have a significant impact on biogeochemical processes and dissolved oxygen concentration in the water column (Allahdadi, Jose, and Patin, 2013; Chaichitehrani, 2012; Chaichitehrani *et al*., 2014; Tehrani *et al*., 2013; Wiseman *et al*., 1997). Hence, the understanding of hydrodynamics induced by a hurricane is vital for studying coastal erosion and water quality on the continental shelf.

Many studies have examined the hydrodynamic response to hurricanes in the northern Gulf of Mexico. Some studies focused on hurricane storm surges and wave field (Cardone, Cox, and Forristall, 2007; Rego and Li, 2009, 2010; Siadatmousavi *et al*., 2012). Currents and sediment transport induced by hurricanes in the northern Gulf of Mexico have been addressed by several studies based on both observations and numerical simulations (for example, Cooper and Thompson, 1989a,b; Keen and Glenn, 1999; Ly, 1994; Miner *et al*., 2009; Mitchell *et al*., 2005; Teague *et al*., 2007; Xu *et al*., 2016). Ly (1994) studied water levels and currents induced by Hurricane Frederic using a 3-D finite-difference ocean model with a sigma coordinate in the vertical. Hurricane Frederic made its landfall at Dauphin Island, Alabama, on 12 September 1979, producing currents of up to 2 m/s as well as inertial motions on the shelf in the northern Gulf of Mexico. Hurricane Ivan passed over an array of 14 acoustic Doppler current profilers (ADCPs) deployed at the edge of the continental shelf off Mobile, Alabama, in September 2004, which provided a unique opportunity to study the response of inner- and outer-shelf water in this area to a hurricane. Mitchell *et al*. (2005) and Teague *et al*. (2007) analyzed time series data for water level and current velocity and found that the outer-shelf response to the hurricane followed the same four stages suggested by Pedlosky (1979) and Price, Sanford, and Forristall (1994). These stages are defined by the magnitude and direction of hurricane wind and are

DOI: 10.2112/JCOASTRES-D-16-00129.1 received 19 July 2016; accepted in revision 3 January 2017; corrected proofs received 28 February 2017; published pre-print online 18 April 2017.
*Corresponding author: nabiallahdadi@gmail.com

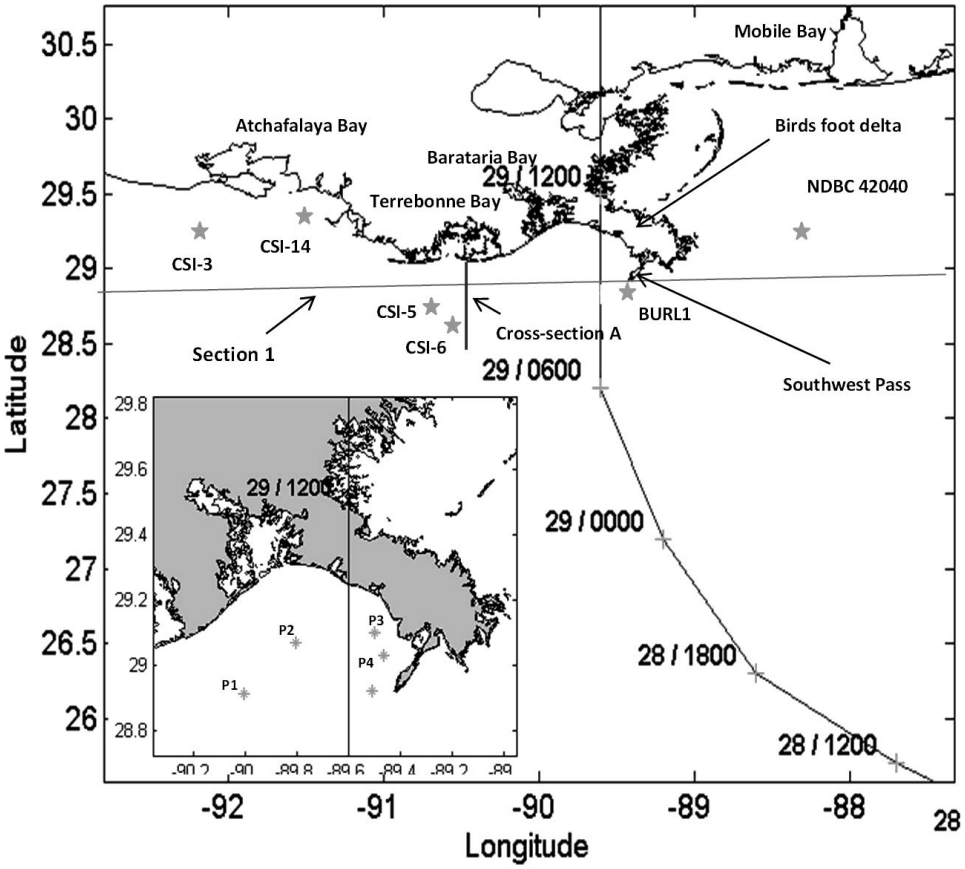

Figure 1. Track of Hurricane Katrina in the northern Gulf of Mexico at different dates and times. Asterisks show the locations of wind and current measurement stations, where simulated time series of current and water level are also presented. Locations of E-W cross section (Section 1) and N-S cross section (Cross section A), for which temperature profiles are presented in Figures 13 and 14, are shown by solid lines.

functions of both the hurricane eye's location on the shelf and the radius of maximum wind (Mitchell *et al*., 2005). On the edge of the shelf, the largest currents were recorded by the current meters to the left of the hurricane's eye, while on the outer shelf, the largest current was measured to the right of the hurricane track. The large near-bottom currents caused substantial scours at a depth of 90 m below the surface.

Hurricane Katrina was one of the most devastating hurricanes in U.S. history with respect to the damage it caused. Starting as a tropical depression over the Bahamas on 23 August 2005 (Knabb, Rhome, and Brown, 2005), Katrina upgraded to a Category 5 hurricane on 28 August after passing over warm waters associated with the Loop Current (Shen *et al*., 2006). The hurricane degraded as it approached the Louisiana shelf. In the morning (GMT time) of 29 August, as a Category 3 hurricane, Katrina made its first landfall in the northern Gulf of Mexico between Grand Isle, Louisiana, and the Mississippi River mouth. Figure 1 shows the track of Hurricane Katrina as it traveled in the northern Gulf of Mexico.

Several modeling studies focused on the effect of storm surges and waves generated by Katrina (Cardone, Cox, and Forristall, 2007; Chen, Wang, and Tawes, 2008; Chen, Wang, and Zhao, 2009; Dietrich *et al*., 2011; Wang and Oey, 2008); however, few studies focused on circulation. A modeling study of Katrina's current hydrodynamics was implemented by Wang and Oey (2008) using the Princeton Ocean Model. They found that, as a result of the high forward speed of Katrina, the inertial amplitudes of currents were much larger on the right side of the storm compared with the left side. The study, however, presented a general feature of Katrina's induced currents in the Gulf of Mexico, and the main focus was not on the Louisiana shelf and shallow-water effects. Cardone, Cox, and Forristall (2007) carried out another modeling study using the Advanced Circulation Model (ADCIRC)-2D model for simulating currents in the Gulf of Mexico during Katrina. Although the study shed some light on the general circulation produced by Katrina in the gulf, no specific information on the circulation of the inner Louisiana shelf was presented, similar to the study of Wang and Oey (2008).

In the present paper, the 3-D Finite Volume Community Ocean Model (FVCOM) was used to study the hydrodynamics of Hurricane Katrina, focusing on the current velocity structure and characteristics induced by the hurricane over the Louisiana shelf. Compared with previous studies, the present study benefits from a flexible computational mesh, a

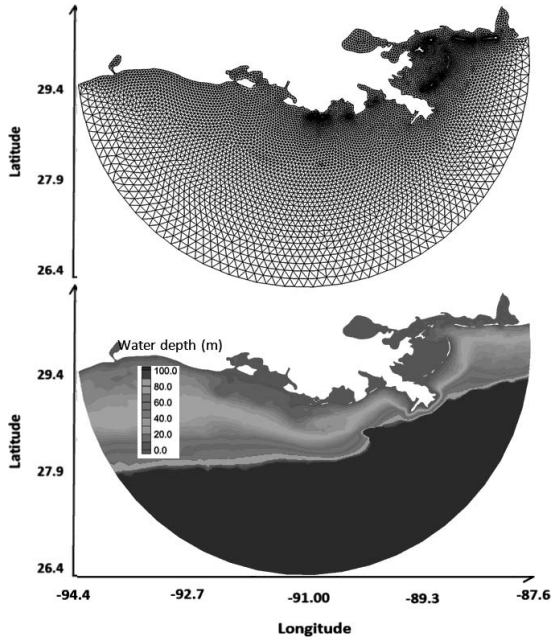

Figure 2. Computational mesh (upper panel); model bathymetry (lower panel).

main focus on the Louisiana shelf, and evaluation of model ability using several water level and current measurements over the inner shallow shelf.

METHODS

Katrina's induced circulation was mainly studied using results from a numerical model verified with field data. Model setup, input data, and model verification are described here.

Model Setup

In the present study, circulation with salinity and temperature variations was simulated using FVCOM, which is a prognostic, unstructured-grid, finite-volume, free-surface, three-dimensional primitive equations ocean model. The model was developed by Chen, Beardsley, and Cowles (2006). The modeling area comprises the coastal, shelf, and deep-ocean regions from approximately Mobile, Alabama, to Galveston, Texas. The computational mesh and bathymetry used in this study are shown in Figure 2. Mesh resolution varies from 10 km along the offshore boundary to about 500 m over the inner shelf. In the vertical direction, 25 sigma layers with higher resolutions at the surface and bottom were considered. Since the main objective was to examine the effect of Hurricane Katrina on shelf circulation without any other external forces, no out-shelf boundary condition was prescribed along the open boundary. Instead, a radiative boundary condition based on an explicit Orlanski radiation condition (Chen, Beardsley, and Cowles, 2006) was used to treat the model open boundary. In order to damp the waves and suppress disturbances, a series of sponge layers was considered with defined damping factors. Based on the Courant-Friedrichs-Lewy (CFL) stability criteria model, external and internal time steps were assumed to be 6 seconds and 60 seconds, respectively. The model was forced with Katrina's wind field from the National Oceanic and Atmospheric Administration (NOAA) Hurricane Research Division Wind Analysis System (H-WIND) database, with background wind from NCEP/NARR (see below for references and more discussion of H-WIND).

Hurricane Wind Field

The high-resolution hurricane wind from H-WIND (Powell, Houston, and Reinhold, 1996; Powell *et al*., 1998) was used for Katrina's wind field. This wind field was produced using available surface weather observations, including ships, buoys, coastal platforms, surface aviation reports, and reconnaissance aircraft data adjusted to the surface. The final wind field was represented at a 10 m height on a 1000 km $\times$ 1000 km moving "box" with spatial resolution of about 6 km centered at the hurricane's central position (Dietrich *et al*., 2011; Wang and Oey, 2008). For this study, hurricane wind field was blended with the NCEP/NARR wind at a 36 km resolution (Allahdadi *et al*., 2011) to include the background winds away from the hurricane center. The algorithm simply used a smooth variation of wind velocity between the border of the H-WIND box and the nearest NCEP/NARR cell so that, out of the H-WIND box, NCEP/NARR dominates. Wind speed and direction obtained from this approach were compared with observations from several stations on the shelf. Satisfactory agreements were found based on the calculated root-mean-square (RMSE) and correlation coefficient (R^2) (Tehrani *et al*., 2013) for different stations, especially for stations west of the Birdsfoot Delta (Figure 3). Snapshots of the produced hurricane wind field for different times are shown in Figure 4.

Wind Friction Coefficient

Wind stress is calculated by the quadratic law:

$$\tau = C_{\mathrm{d}} \rho_{\mathrm{a}} U^2 \quad (1)$$

where, C_{d} is the drag coefficient, ρ_{a} is the air density, and U is wind speed. The drag coefficient is assumed to be dependent on wind speed. Large and Pond (1981) suggested that the drag coefficient increases linearly with wind speed values between 11 m/s and 25 m/s. For wind speeds greater than 25 m/s, the coefficient was considered constant. Although this approach was used in many studies and produced acceptable results, further studies on air-sea interaction and the wind-wave boundary layer showed that the rate of energy transfer from wind to the water surface decreases when the wind speed is larger than a threshold (25–32 m/s) (Makin, 2003, 2005). When the wind speed is greater than the threshold, whitecaps produced at the sea surface prevent further transfer of wind energy to water. Based on this finding, a modified relationship between the drag coefficient and wind speed was determined and selected for calculating Katrina's wind shear.

Model Verification

During Katrina, several -Wave-Current-Surge Information System (WAVCIS; see Stone *et al*., 2009) stations were operational, but most of them failed to measure currents when

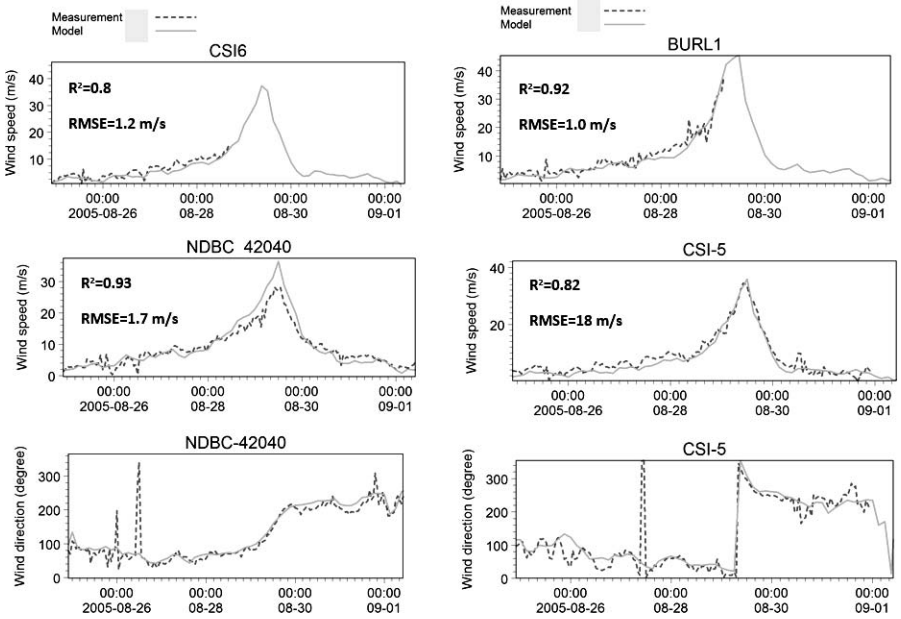

Figure 3. Comparison between the wind data obtained by blending H-WIND and NCEP/NARR and measured wind speeds and directions over the Louisiana shelf.

Katrina was over the shelf. Only station CSI-6, with water depth of 20 m (Figure 1), measured current data for several days before the hurricane reached the Louisiana shelf and for several hours when Katrina was on the shelf. Water-level data during Katrina was obtained at CSI-5 (water depth = 7 m), CSI-3 (water depth = 5 m), and CSI-14 (water depth = 3 m) (see Figure 1 for locations).

Model test runs were implemented for two overall scenarios: (1) an initially unstratified water column and (2) a prestratified water column. For the prestratified case, vertical profiles of temperature and salinity were obtained from the climatological NOAA profiles for the month of August over the Louisiana shelf (NOAA, 2016). Considering a prestratified water column can result in different simulated currents in comparison with the initially unstratified case (Figure 5). All simulations were implemented for a 2-week period from 23 August 2005 to 6 September 2005. Vertical eddy viscosity (Keen and Glenn, 1998) and bottom friction were considered as the calibration parameters. Sensitivity test runs showed that, compared with vertical eddy viscosity, bottom friction had minor effects on changing simulated velocity and water levels under Katrina. Hence, vertical eddy viscosity was further examined to achieve the best agreement with measurements. Constant values for the vertical eddy viscosity as well as a turbulent closure (Mellor-Yamada level 2.5) for calculating this parameter were tested. The best agreement with the WAVCIS data was obtained for the case assuming a prestratified water column along with turbulent closure for vertical eddy viscosity. Therefore, this modeling case was used for examining shelf currents in the results section.

Figures 6 and 7 show the comparison between modeled and measured water levels and velocities at different stations over the shelf. Current measurements at CSI-6 are only available up to the morning of 29 August 2005, when the ADCP stopped working. Since the present modeling only includes wind (no tide is included in order to investigate the effect of the hurricane alone), measured currents were de-tided and compared with simulation results. The tidal analysis tool of Mike 21 was used for tidal analysis of currents (DHI, 2015). For de-tiding the current data, 36 tidal constituents, including the main deepwater constituents of M2, S2, K1, and O1, along with other deep- and shallow-water constituents, were used. Currents were compared for both surface water and water of 5 m from the bottom (total water depth is about 20 m). For these two depths and both the U (E-W) and the V (N-S) current components, currents were in phase and followed the same variations just before the hurricane produced the maximum currents over the shelf. Fortunately, the peak of the hurricane effect on the shelf was well captured by all of the three above-mentioned water level stations. The simulated water level at CSI-5 (located just north of CSI-6 and about 150 km west of the Birdsfoot Delta) reproduced a 0.8 m water level drop induced by the hurricane, which is consistent with measurements. At other stations, including CSI-14 and CSI-3, the model appropriately simulated water level variations induced by the hurricane. However, larger fluctuations and differences were observed for simulated water level at these two stations. It could be due to the shallow depth of the Atchafalaya Bay and the area of the mouth.

An index of agreement (d) proposed by Willmott (1981) was used for quantification of model performance in the simulation of currents and water level. The index is represented as

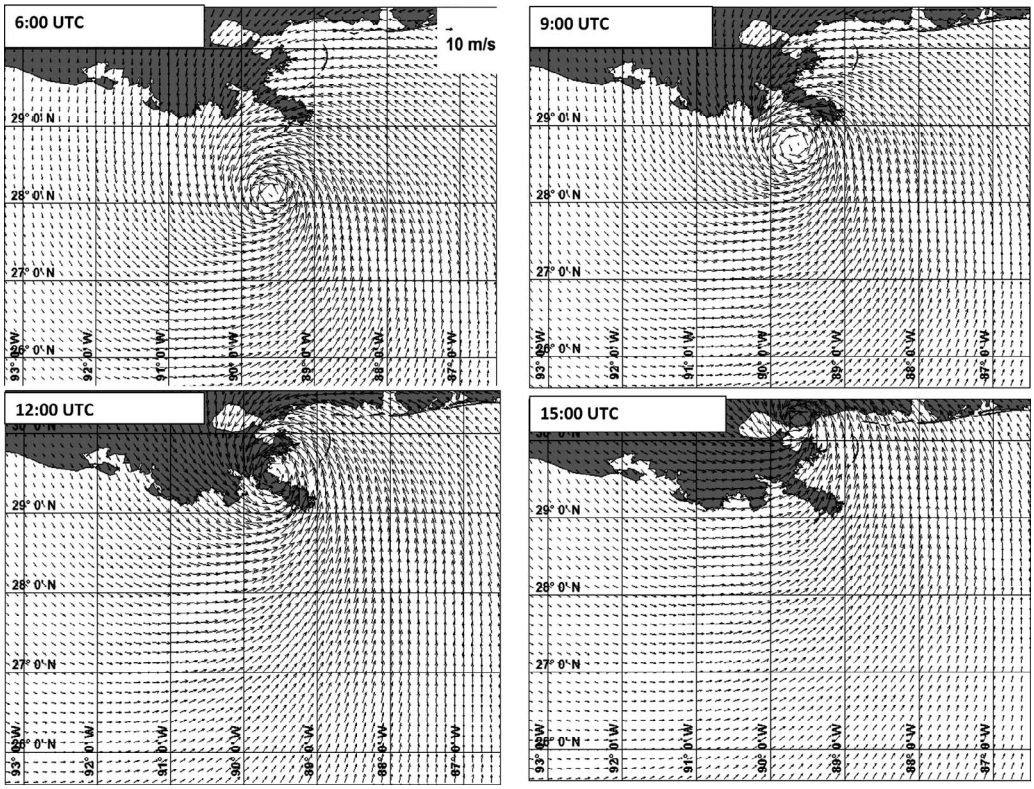

Figure 4. Katrina's wind field over the Louisiana shelf on 29 August 2005, used for hydrodynamics simulation at different times.

$$d = 1 - \frac{\sum_{j=1}^{n} [y(j) - x(j)]^2}{\sum_{j=1}^{n} [|y(j) - \bar{y}| + |x(j) - \bar{x}|]^2} \quad (2)$$

where, *x(j)* refers to measured values, *y(j)* refers to simulated values, and $\bar{x}$ and $\bar{y}$ represent the mean values of measurement and simulation, respectively. Index values vary between 0 for poor agreement and 1 for a perfect match. Table 1 shows the values of the index for all model validations shown in Figures 6 and 7.

Due to the lack of conductivity, temperature, and depth (CTD) or moored data for temperature and salinity for the days before, during, and after Katrina, it was not possible to evaluate the simulated temperature and salinity across the water column and over the Louisiana shelf. The only available data was sea surface temperature measured by satellites. However, the extensive cloud coverage during the hurricane contaminated satellite measurements of sea surface temperature (SST) using Moderate Resolution Imaging Spectroradiometer (MODIS) and Advanced Very High Resolution Radiometer (AVHRR). This is because the measurements are based on infrared and midinfrared wavelength bands, which are absorbed by the abundant atmospheric water vapor during hurricanes. Since water vapor is transparent to microwave bands, SST derived by them can be used for the hurricane period. The Microwave Optimally

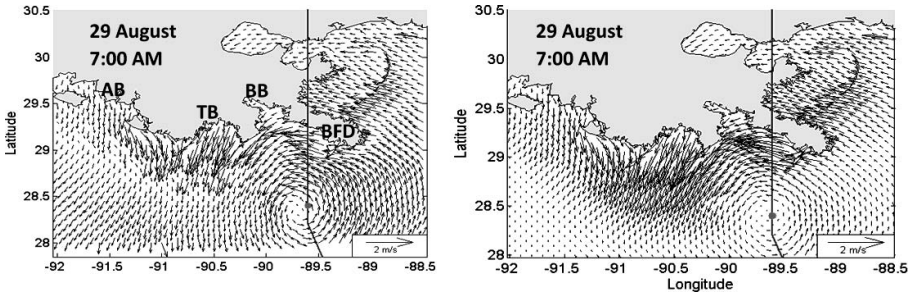

Figure 5. Sample simulated currents for the prestratified (left) and unstratified (right) water column.

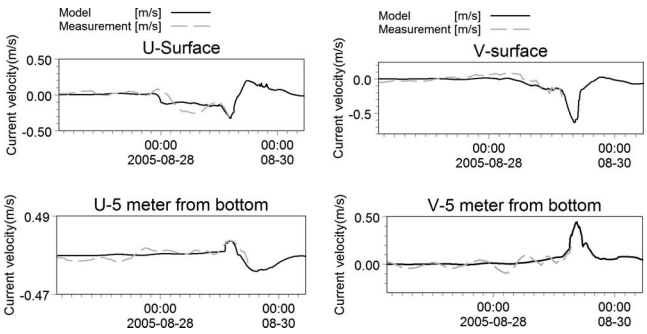

Figure 6. Comparison between simulated and measured currents at CSI-6.

Interpolated (MW-OI) SST is reliable for model evaluation (Pan and Sun, 2013; Reynolds and Smith, 1994). Data is accessible from the Remote Sensing Systems Web site (www.remss.com). Regarding the measurement limitations, data are only available over the offshore areas extended roughly to the shelf break in the northern Gulf of Mexico. The data closest to the inner Louisiana shelf were used for model calibration/evaluation. Figure 8 shows an example of comparisons between MW-OI sea surface–derived temperatures for the shelf break region and similar quantities from a calibrated model at 0830 on 30 August 2005. The calibrated model parameters are consistent with the best results for hydrodynamics. The cooler areas on the right side of Katrina's track suggest rightward bias, which was appropriately simulated by the model.

RESULTS

Model outputs from the simulation case that resulted in the best agreement with measurements (prestratified water column with a turbulent closure for vertical eddy viscosity) were used for further examining shelf currents during Katrina. The simulated near-surface (1 m below the surface) velocity vectors are presented in Figure 9 for different times on the morning of 29 August 2005 (UTC time), when Hurricane Katrina was approaching the Birdsfoot Delta and made its landfall. Results showed that at 0700 UTC, surface currents over the deep water S of the Birdsfoot Delta followed a spatial pattern similar to that of the hurricane wind. A cyclonic gyre was created under the hurricane with N currents to the E of the track and S currents to the W, implying a predominant effect of wind stress on near-surface currents. The strongest currents were observed at locations E of the hurricane track, which was consistent with the right-front–quadrant intensification due to the forward movement of the hurricane (*e.g.*, Church, Joyce, and Price, 1989; Price, Sanford, and Forristall, 1994; Sanford *et al.*, 1987). As a Category 4 hurricane at that time, Katrina strongly affected surface currents over the shallow Louisiana shelf, including areas off the Barataria and Terrebonne Bays, where southwestward to S currents reached the speed of 1 m/s. The inner Louisiana shelf was located on the left side of Katrina's track at this time and prior to the final landfall. Hence, as a result of persistent N to NE hurricane winds, S to southwestward currents were dominant over the shelf during

Table 1. *Willmott indices for different stations.*

Station	*U* (surface)	*V* (surface)	*U* (bottom)	*V* (bottom)	Water Level
CSI-6	0.89	0.80	0.79	0.75	—
CSI-5	—	—	—	—	0.97
CSI-3	—	—	—	—	0.85
CSI-14	—	—	—	—	0.87

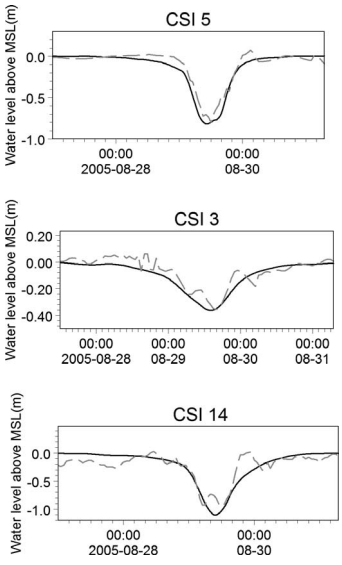

Figure 7. Comparison between measured and simulated water levels at different stations over the shelf.

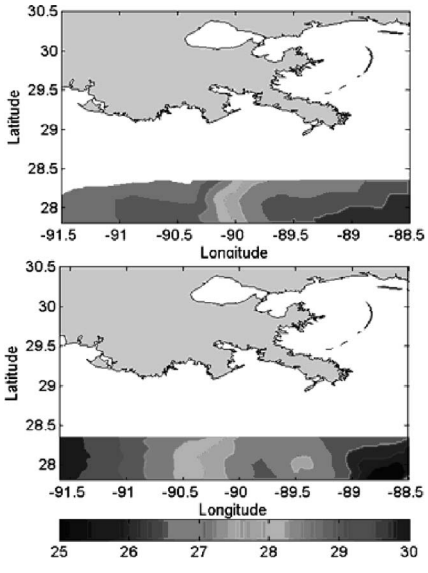

Figure 8. Sea surface temperature measured by satellite (MW-OI product) at 8:30 on 30 August 2005 along the Louisiana shelf-break (upper panel) and simulated SST at the same time (lower panel).

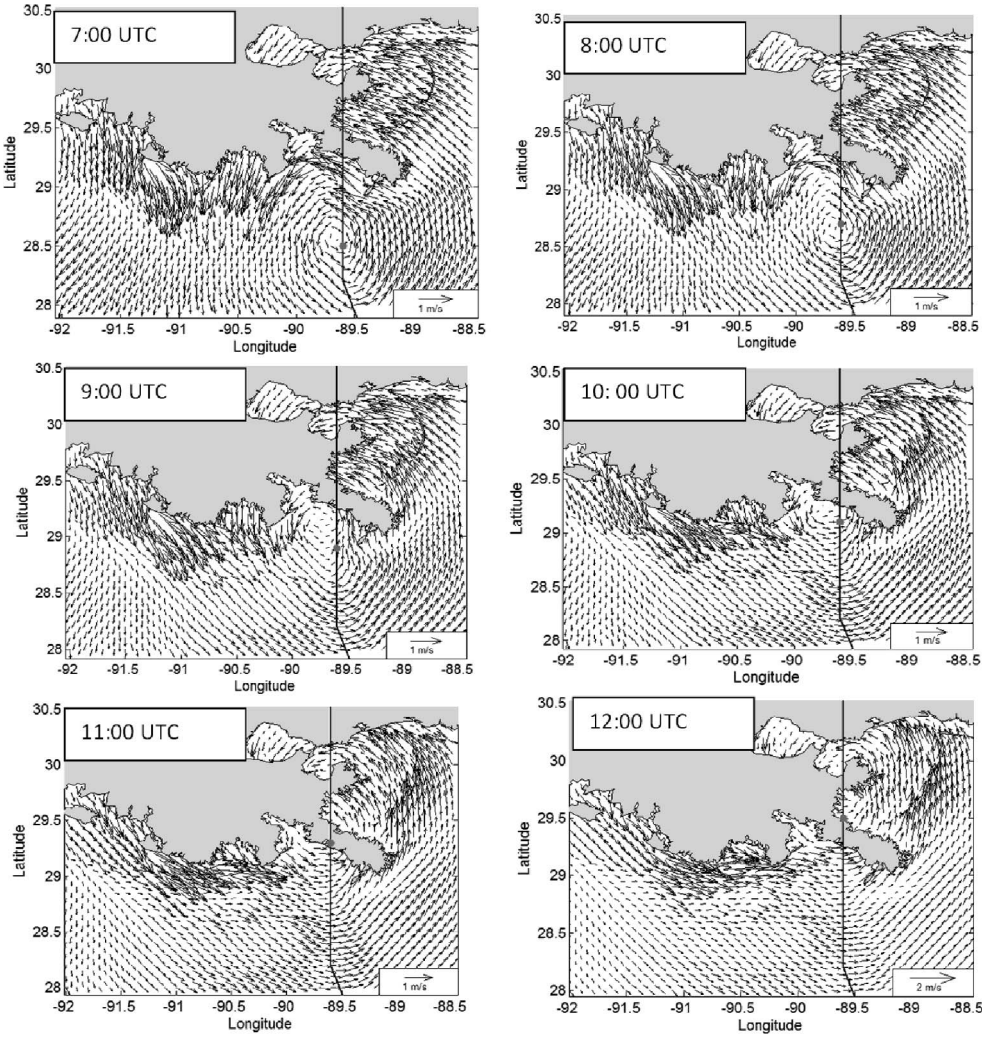

Figure 9. Simulated near-surface currents induced by Hurricane Katrina at different hours on 29 August 2005 (the solid line represents the hurricane's track and the circle shows the location of the hurricane's eye).

the hours that Katrina was passing over the outer and inner shelves.

The shallow shelf E of the delta was also affected by the strong E winds from the hurricane. The area experienced relatively strong W currents. As Katrina progressed N within the next 2 hours, it was about to degrade to a Category 3 hurricane, and there was a general decrease in current speeds.

At 0900 UTC, when the eye was located just southwestward of the Birdsfoot Delta, strong NW currents with speeds up to 1.5 m/s were generated along the W side of the delta. During the next 2 hours, the direction of currents were changed W and then southwestward following the hurricane's wind field structure, while the maximum velocity decreased to less than 1 m/s.

At the time of the first landfall at Grand Isle, the response of the shelf W of the delta was a cyclonic gyre exhibiting stronger currents on the W side. At the same time, NW currents parallel to the Birdsfoot Delta appeared E of the delta and were extended over the entire E shelf during the next hour.

At 1100 UTC, the surface currents at the mouth of Terrebonne Bay and further offshore veered SE as a result of the wind direction change as the hurricane moved, while currents off Barataria Bay remained S due to its proximity to the hurricane track. At 1200 UTC, surface currents in front of Terrebonne Bay completely turned to the E, while off Barataria Bay the surface currents changed directions to the E and SE.

Contrary to the near-surface currents (Figure 9) that generally followed the hurricane wind pattern, the near-bottom currents (about 3 m above the bottom, Figure 10) were less consistent with the wind field, both temporally and spatially. Over both inner and outer shelves, the surface- and bottom-water currents often showed reversed directions. At 0700 UTC, the deepwater response to the cyclonic near-surface gyre (thereby to the hurricane wind field) generated offshore of the Birdsfoot Delta was an anticyclonic gyre with stronger currents

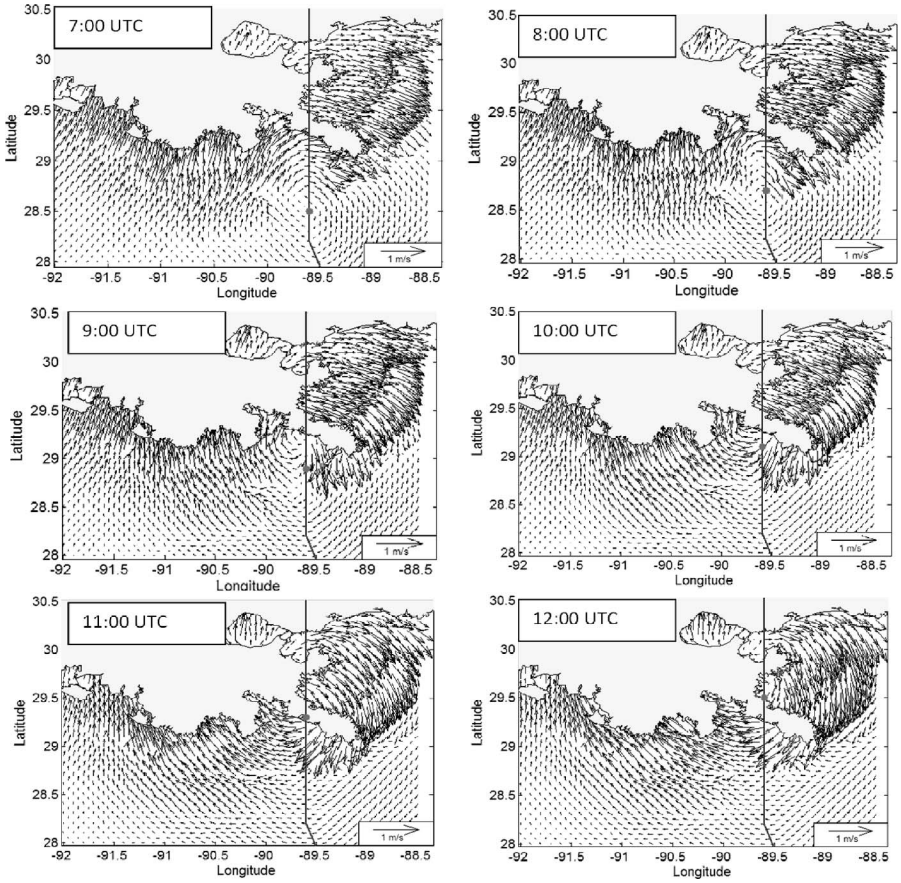

Figure 10. **S**imulated near-bottom currents induced by Hurricane Katrina at different hours on 29 August 2005 (11:00 is the landfall time over the Birdsfoot Delta).

on the E side. Over the Louisiana shelf and at the shelf break, currents were generally N with the maximum current speeds about 0.6 m/s at the Terrebonne Bay entrance. Offshore of Barataria Bay, currents veered NE and became a part of the W limb of an anticyclonic gyre over the shelf W of the Birdsfoot Delta, where maximum current speed reached 0.4 m/s. The Louisiana shelf W of the Birdsfoot Delta was not the only inner-shelf area with bottom currents flowing in the reverse direction of surface currents. Bottom currents over the shallow shelf E of the delta also showed reverse directions compared with near-surface currents. At 1100 UTC, when the hurricane's eye was located approximately 20 km W of the Southwest Pass, coastal and offshore bottom currents at Barataria and Terrebonne Bays and further W at Atchafalaya Bay completely turned to the N. The anticyclonic bottom gyre previously formed W of the Birdsfoot Delta was substantially decreased in size and was confined between the delta, shelf break, and the N current flowing toward Barataria Bay. The gyre almost disappeared at 1200, the time of the final landfall. Southwestward deepwater currents up to 0.6 m/s were produced along the delta at this time. The response of bottom currents offshore of Barataria Bay at this time was NW flow reaching a maximum speed of 0.4 m/s, while currents over Terrebonne Bay and its offshore areas did not change much. The bottom currents generated over the shallow E shelf at this time were mostly SE to S. Along with the southwestward current S of the delta and the NW current at the mouth of Barataria and Terrebonne Bays, the current over the E shelf formed an anticyclonic gyre whose E and W limbs were separated by the Birdsfoot Delta. At two different times when the hurricane's eye was present over the outer and inner shelves, the average direction of surface and bottom currents over different regions of the inner shelf are compared and contrasted in Table 2.

In order to examine the temporal variations of currents induced by Katrina over the Louisiana shelf, time series of simulated surface currents are presented at several locations (see Figure 1 inset for locations). These locations were selected from both sides of the hurricane track, including two stations on the left and two stations on the right. Figure 11 shows the surface-current time series at different locations. Results were examined from 24 August, almost 5 days before the eye reached the shelf, to 2 September, about 4 days after the landfall.

Station P1 is located off Barataria Bay about 45 km (1.2 times the radius of maximum wind, or R_{mw}) W of the track, where the water depth is about 33 m. During the time that this location was being affected by hurricane winds (28–30 August),

Table 2. *Average directions of surface and bottom currents over different regions on the Louisiana shelf for two different locations of Katrina.*

Region	Surface	Bottom
29 August, 0700 (UTC)		
Off Atchafalaya Bay	S	NE
Off Terrebonne Bay	S to SW	N to NE
Off Barataria Bay	SW	NE
Off the Birdsfoot Delta	NW	SE
West of the Birdsfoot Delta	W	E
29 August, 1100 (UTC)		
Off Atchafalaya Bay	SE	N
Off Terrebonne Bay	S	N
Off Barataria Bay	SW	N
Off the Birdsfoot Delta	N	S
West of the Birdsfoot Delta	NW	NW

southwestward to SE currents with speeds up to about 0.7 m/s were produced. The specific location of the point at the left side of the track caused a counterclockwise temporal rotation of current vector. After the landfall (after 30 August), hurricane-induced currents were followed by some weak shelf oscillations with speeds of less than 0.1 m/s. These daily inertial motions were produced as a result of resonance between posthurricane winds stresses and the Coriolis force and are one of the prominent hydrodynamic features associated with passing tropical storms (Wang and Oey, 2008). Similar oscillations were reported at the shelf break and inner continental shelf of the northern Gulf of Mexico as a result of Hurricane Frederic (Ly, 1994).

For station P2, which is also located on the left side of the track but at a distance of 0.6 R_{mw} from the eye and S of Barataria Pass (depth ~30 m), the overall temporal variations of velocity were similar to those at station P1, *i.e.* showing a counterclockwise rotation of flow and a peak in current speed almost at the time that the eye was closest to the station. The maximum velocity of about 0.5 m/s was smaller than that at station P1, which can be attributed to its location. Similar to P1, inertial currents were present at P2 after the landfall.

The velocity variations on the right side of the track were substantially different both in magnitude and direction from those at P1 and P2. The maximum current speed at station P3 was about 1.8 m/s. This station is located on the right side of the track midway between the Birdsfoot Delta and the hurricane track, about 0.3 R_{mw} from the track (depth 20 m). Unlike the left side of the hurricane track, the velocity vector rotated in the clockwise direction.

A similar pattern was observed for variations in currents at station P4, located NW of the Southwest Pass with water depth of 16 m. The maximum current speed at this station was more than 2.2 m/s. There are two reasons for the increased velocity at these stations located on the right side of the track: first, the rightward bias as a result of the superposition of clockwise wind vector on the right side of the eye and the movement of the hurricane; and second, the effect of the Birdsfoot Delta as a confining boundary.

Temporal rotation of current vectors at each side of Katrina's eye and associated current magnitudes, especially corresponding to peak currents at each station, are consistent with measured and simulated results during Hurricane Andrew of 1992, which made landfall over the Atchafalaya Bay Delta (Keen and Glen, 1998). Keen and Glen reported current magnitudes of up to 1 m/s and 2 m/s over the inner Louisiana shelf for the left and right sides of Andrew's track, respectively, with temporal rotation of current vectors similar to the results from Katrina.

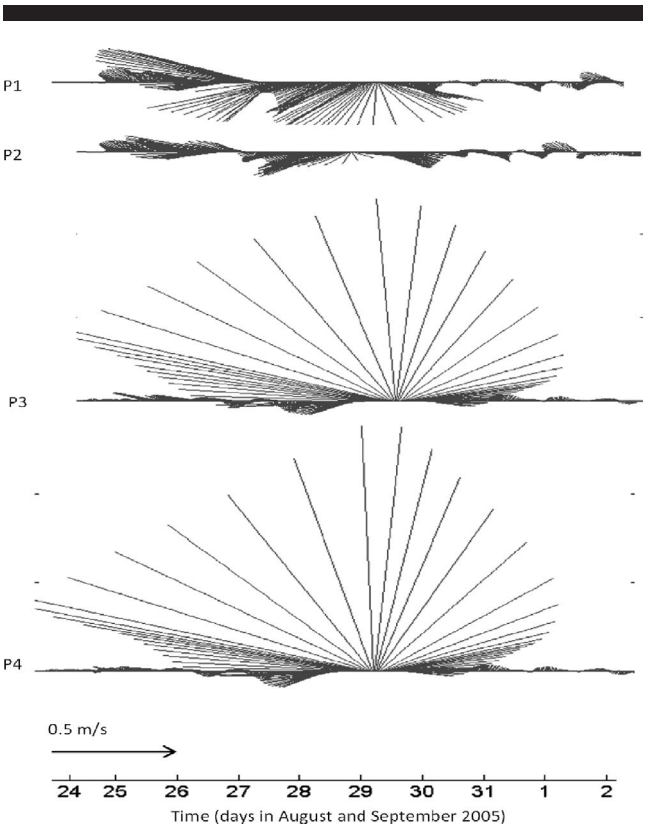

Figure 11. Time series of simulated surface currents at different locations over the shelf.

The clockwise/counterclockwise rotation of the current vector during the hurricane for locations at the right and left of the hurricane track is due to the specific characteristic of the hurricane-induced wind field that is produced by a combination of the hurricane cyclonic rotation in the Northern Hemisphere and its simultaneous forward motion (Wang and Oey, 2008; Allahdadi, 2015).

DISCUSSION

Hydrodynamic response of shelf circulation is quite complicated during a hurricane (Ly, 1994; Mitchell *et al*., 2005). The response is a function of the hurricane track, its forward speed, and the maximum sustained wind speed (Mitchell *et al*., 2005; Wang and Oey, 2008). The response can be associated with reversal of current directions in the vertical, which may suggest either a pressure gradient–induced return flow or a baroclinic response. For the simulated currents over the Louisiana shelf during Katrina, the reversal of currents is consistent with previous studies (Cooper and Thompson, 1989a,b; Mitchell *et al*., 2005; Teague *et al*., 2007).

During a hurricane the generated current field is the result of momentum balance between the local acceleration, wind forcing, the Coriolis force, the external pressure gradient,

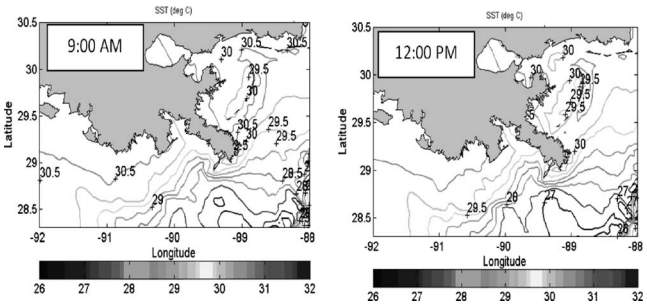

Figure 12. Simulated SST over the Louisiana shelf for two different positions of Katrina on the shelf on 29 August 2005.

bottom friction, and stratification (Keen and Glen, 1998). This is illustrated by examining the horizontal momentum equations for a 3-D system:

$$\frac{\partial \boldsymbol{u}}{\partial \boldsymbol{t}} + \boldsymbol{u}\frac{\partial \boldsymbol{u}}{\partial \boldsymbol{x}} + \boldsymbol{v}\frac{\partial \boldsymbol{u}}{\partial \boldsymbol{y}} + \boldsymbol{w}\frac{\partial \boldsymbol{u}}{\partial \boldsymbol{z}} - \boldsymbol{fv} = -\frac{1}{\boldsymbol{\rho}_0}\frac{\partial \boldsymbol{P}}{\partial \boldsymbol{x}} + \frac{\partial}{\partial \boldsymbol{z}}\left(\boldsymbol{K_m}\frac{\partial \boldsymbol{u}}{\partial \boldsymbol{z}}\right) + \boldsymbol{F}_u \tag{3}$$

$$\frac{\partial \boldsymbol{v}}{\partial \boldsymbol{t}} + \boldsymbol{u}\frac{\partial \boldsymbol{v}}{\partial \boldsymbol{x}} + \boldsymbol{v}\frac{\partial \boldsymbol{v}}{\partial \boldsymbol{y}} + \boldsymbol{w}\frac{\partial \boldsymbol{v}}{\partial \boldsymbol{z}} + \boldsymbol{fu} = -\frac{1}{\boldsymbol{\rho}_0}\frac{\partial \boldsymbol{P}}{\partial \boldsymbol{y}} + \frac{\partial}{\partial \boldsymbol{z}}\left(\boldsymbol{K_m}\frac{\partial \boldsymbol{v}}{\partial \boldsymbol{z}}\right) + \boldsymbol{F}_v \tag{4}$$

In the above equations, parameters are defined as follows: x, y, z: E-W, N-S, and vertical Cartesian coordinate axes, respectively; u: current velocity component in x-direction; v: current velocity component in y-direction; t: time; f: Coriolis parameter; P: pressure; g: acceleration of gravity; ρ: water density; K_m: vertical eddy viscosity coefficient; and F_u, F_v: other forces including wind stress, bottom stress, and horizontal momentum diffusion terms.

At the left-hand side of the equations, $-fv$ and fu account for the Coriolis force, while other terms represent acceleration. On the right side, the first term shows the effect of the pressure gradient. The second term on the right-hand side of each equation accounts for the effect of vertical momentum flux on currents in each x and y direction. This term is a function of the vertical eddy viscosity, which is controlled by stratification across the water column.

The contribution of each component to currents depends on the hurricane category, relative location with respect to the eye, stratification characteristics, and the shelf bathymetry. In some cases, for the remote areas at the left side of the hurricane's eye with weak wind stress, currents are mostly the result of interplay between surface stress and pressure gradient (Keen and Glenn, 1998). In the case of a strongly stratified water column, the downward surface wind-energy penetration is regulated by the stratified layers, and a different circulation pattern is produced compared with a nonstratified or weakly stratified water column (Csanady, 1972; Zhang and Steele, 2007). In this case, intense hurricane winds produce a surface mixed layer with an almost-uniform current velocity across the mixed-layer depth (Elsberry, Fraim, and Trapnell, 1976). A lower stratified layer starting at the base of the mixed layer is

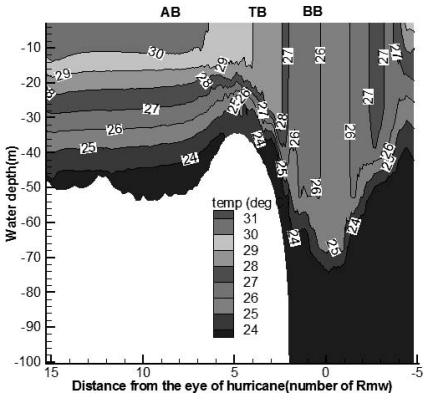

Figure 13. Vertical temperature structure across an E-W section over the Louisiana shelf at 10:00 on 29 August 2005 (Section 1 in Figure 1). Locations of the Barataria Bay, the Terrebonne Bay, and the Atchafalaya Bay are identified by BB, TB, and AB, respectively.

associated with high spatially variable temperature/salinity. This is basically a two-layer circulation system that forms a baroclinic circulation across the water column (Ly, 1994).

On the continental shelf and shelf break, the response to hurricanes can be either barotropic or baroclinic, depending on the intensity and location of the hurricane (Cooper and Thompson, 1989b; Mitchell *et al*., 2005; Teague *et al*., 2007). The baroclinic and barotropic response of oceanic/shelf waters are mainly defined based on the 3-D density field. The primary condition for a barotropic response is spatially uniform density, while for a baroclinic response density should change with depth and horizontal position (Stewart, 2009). Regarding the flow pattern, the barotropic response causes a vertically homogeneous flow (Ly, 1994).

For several Category 4 and 5 hurricanes, it was reported that the region within 1 R_{mw} from the center of the hurricane showed a barotropic response over shallow waters (Keen and Glenn, 1999; Teague *et al*., 2007). The intense hurricane wind mixes the water column and completely destroys the stratification. As a result, the surface Ekman layer merges with the bottom boundary layer, causing a barotropic response (Mitchell *et al*., 2005). Outside of this interior region, mixing is weaker and the stratification cannot be completely destroyed; hence a baroclinic response is produced. Regarding the above description of barotropic and baroclinic response, both hydrodynamics and 3-D variations of density for the Louisiana shelf were examined to determine the dominant response to Katrina. The spatial variation of density was investigated as the first criterion. Figure 12 shows the spatial variations of simulated SST over the shelf for the two different times that Katrina's eye was present south of the delta or on the shelf. Asymmetric SST variations resulted due to the corresponding asymmetric hurricane force, with SST varying between 28°C right at the west side of the Birdsfoot Delta to about 31°C off the Atchafalaya Bay, about 200 km to the west of the eye. Simulated sea-surface salinity (not shown) follows similar patterns. Shelf-wide variations of water temperature across the water column for the time that the eye was right at west of

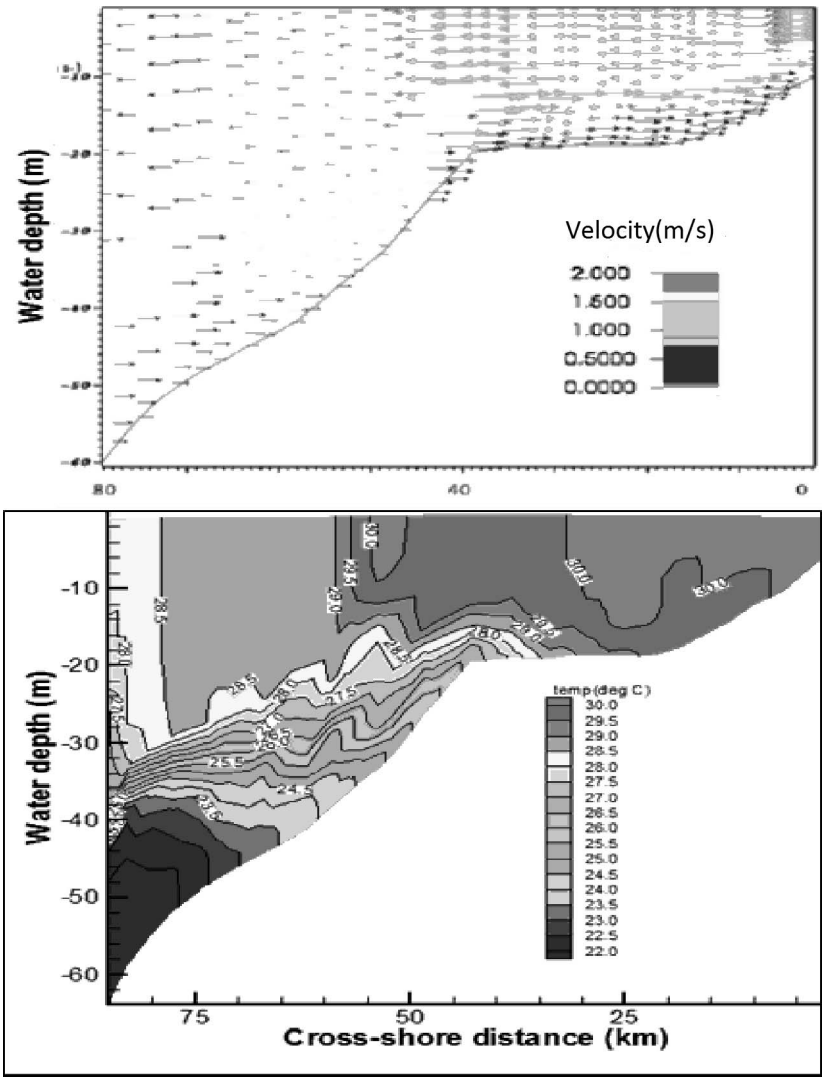

Figure 14. Upper panel: vertical pattern of simulated currents induced by Katrina across a N-S transect in front of Terrebonne Bay (Cross section A in Figure 1) when the eye is located west of the Birdsfoot Delta. Lower panel: the corresponding simulated temperature response.

the delta for an E-W cross section (Figure 1, Section 1) are shown in Figure 13. The figure shows that at this time the temperature/salinity stratification (and, as a result, density stratification) increases over the shelf area as the distance from the eyes increases. This shelf-wide stratification for areas out of 1 R_{mw} could cause a baroclinic response. The response is further evaluated by considering a N-S cross section (Figure 1, Cross section A), which shows variations in water temperature across the water column and along the cross section at the same time that the temperature data for the E-W cross section were shown (Figure 14, lower panel). The section is located in front of Terrebonne Bay at a distance of about 3.5 R_{mw} from the eye to the left side. Temperature variations for Cross section A show that stratification dominates for water depths larger than 20 m. For a location on this cross section where total water depth was 30 m, the strength of stratification at a depth of 25 m was quantified using the gradient Richardson number (Lyons, Panofsky, and Wollaston, 1964):

$$R_i = \frac{N^2}{\left(\frac{\partial u}{\partial z}\right)^2 + \left(\frac{\partial v}{\partial z}\right)^2} \quad (5)$$

$$N^2 = -\frac{g}{\rho}\frac{\partial \rho}{\partial z} \quad (6)$$

where, R_i is the Richardson number, N is the Brunt-Väisälä or buoyancy frequency (in s^{-1}), ρ is the density of water, and g is acceleration due to gravity. Small Richardson number values correspond to large velocity shear across the water column, under which condition turbulence forces may overwhelm stratification. Increasing the value of the Richardson number above a threshold (0.2–0.25) suppresses turbulence. During

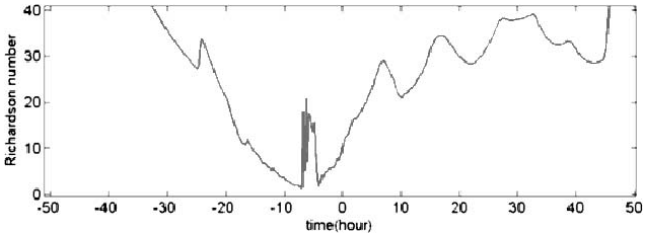

Figure 15. The Richardson number for a point across the water column of Transect A (time 0 is the time that the hurricane's eye is located right west of the Birdsfoot Delta, so negative and positive times indicate before and after that time, respectively).

Katrina and after the landfall, the Richardson number at this location and depth is much larger than the threshold value of 0.25, with a minimum of about 2 that occurred 3–7 hours before the time that the eye reached the western side of the Birdsfoot Delta (Figure 15). The corresponding current at this cross section (Figure 14, upper panel) shows that for the upper part of the water column—where there is a surface mixed layer according to the temperature diagram—current direction is toward the outer shelf, while for the lower stratified part (lower than the approximate depth of 20–30 m, depending on the location along the cross shelf), currents flow shoreward. The above-mentioned behaviors, including horizontal temperature gradient, vertical stratification, and reversal current pattern across the water column, are together evidence of a baroclinic behavior, especially at the location of the studied N-S cross section during Katrina (Ly, 1994; Stewart, 2009). The baroclinic response of the Louisiana shelf to Katrina was strongly a result of the specific track of Katrina and the shelf morphology. Shelf response to the hurricane could be different if the track had been more toward the west, similar to the track of Hurricane Andrew (Keen and Glenn, 1998).When Hurricane Katrina was over the Louisiana shelf, most of the shelf was out of the interior mixed region. Katrina's track divided the shelf into a deeper narrow region to the right, which was confined by the Mississippi Birdsfoot Delta, and a wide, shallower area extending from west of the track to the Atchafalaya shelf. Offshore of Barataria Bay was within 1.2–1.5 R_{mw} from the hurricane center, while Terrebonne Bay and its offshore area were at distance of 2.5–5 R_{mw} from the hurricane center. Over these regions, especially Terrebonne Bay, wind speed and the associated mixing were significantly lower compared with the interior. Hence, the stronger shelf stratification decoupled the surface and bottom Ekman layers.

The inhomogeneous cooling caused by a hurricane (Figure 12 shows Katrina's effect on the Louisiana shelf) can also contribute to the baroclinic shelf response. The vorticity field generated as a result of this inhomogeneous temperature cooling can form anticyclonic gyres beneath the mixed layer after the hurricane has dissipated (Pan and Sun, 2013).

CONCLUSION

In this paper, the hydrodynamic response to Hurricane Katrina over the Louisiana inner shelf and parts of the outer shelf area was examined using a high-resolution FVCOM model verified against field data of current and water level. The model was forced by a combination of H-WIND and NCEP/NARR background wind. Over the Louisiana shelf and the adjacent outer shelf, the near-surface currents were consistent with the hurricane wind field (cyclonic). The bottom water had a reversed circulation (anticyclonic). This two-layered baroclinic response was produced as a result of the specific track of Katrina, whose distance to the major parts of the Louisiana shelf was larger than 1 R_{mw}. Over the Louisiana shelf, Katrina degraded to a Category 3 and then a Category 2 hurricane, and therefore the wind force over the shelf weakened more. Consequently, mixing was not strong enough over the western shelf to completely destroy the stratification. Furthermore, spatial variations of surface cooling induced by a hurricane can produce a horizontal baroclinic pressure gradient that forces anticyclonic gyres beneath the mixed layer. Over the narrow area confined between Katrina's track and the Birdsfoot Delta, shelf geometry and morphology as well as the rightward bias effect of hurricane winds highly intensified currents, thereby producing intense velocity mixing.

The baroclinic hydrodynamics model of hurricane-induced circulation over an inner-shelf area like the Louisiana shelf is of great importance in the numerical study of sediment transport and biogeochemical processes. Over the Louisiana shelf, hurricane season almost coincides with seasonal hypoxia spreading in the northern Gulf of Mexico. Intense hurricane currents are associated with substantial mixing forces and reoxygenation of the water column. Hence, a passing hurricane can degrade the extension of the hypoxic zone. The accurate impact on the size of this zone and associated oxygen concentrations can be determined through a detailed oxygen transport model that uses hydrodynamics results similar to those discussed in this paper. This validated model can also be coupled with a sediment transport model to study the effect of Katrina (or other hurricanes by following the same approach) on the bottom boundary layer dynamics during catastrophic storms. Intense currents generated by hurricane wind highly contribute to resuspension of fine bed sediments over the Louisiana shelf, especially close to the Mississippi River Delta. Furthermore, the baroclinic effect causes reverse currents compared with surface currents. This means that, at the right side of the track, sediment transport could be toward offshore, and onshore sediment transport occurs at the left side. The sediment transport specific to Katrina would be imperative for investigating sedimentation rate at the sand-borrowing sites over the Louisiana shelf for planning dredging operations.

ACKNOWLEDGMENTS

The authors would like to thank Dr. Changsheng Chen (University of Massachusetts-Dartmouth) for his kindness in sharing the FVCOM code. This research was undertaken at the Wave-Current-Surge Information System (WAVCIS) Lab at Louisiana State University. The authors appreciate the support through research grants of Louisiana's Coastal Protection and Restoration Authority, Lake Pontchartrain Basin Foundation, the National Science Foundation (OCE-

0554674, DEB-0833225, OCE-1140268, and OCE-1140307), Stennis Space Center, and NOAA through the Hypoxia Project (NA06NPS4780197 for NGoMEX funded to LUMCON and Louisiana State University, and NA06OAR4320264–06111039 to the Northern Gulf Institute by NOAA's Office of Oceanic and Atmospheric Research, the U.S. Department of Commerce, and Shell). Manuscript edits by Shima Massiha of the Coastal Studies Institute at Louisiana State University are sincerely appreciated.

LITERATURE CITED

Allahdadi, M.N., 2015. Numerical Experiments of Hurricane Impact on Vertical Mixing and Re-stratification of the Louisiana Shelf. Baton Rouge, Louisiana: Louisiana State University, Ph.D. dissertation, 178p.

Allahdadi, M.N.; Jose, F., and Patin, C., 2013. Seasonal hydrodynamics along the Louisiana coast: Implications for hypoxia spreading. *Journal of Coastal Research,* 29(5), 1092–1100.

Allahdadi, M.N.; Jose, F.; Stone, G.W., and D'Sa, E.J., 2011. The fate of sediment plumes discharged from the Mississippi and Atchafalaya Rivers: An integrated observation and modeling study for the Louisiana shelf, USA. *Proceeding of the Coastal Sediments 2011* (Miami, Florida), pp. 2212–2225.

Cardone, V. J.; Cox, A.T., and Forristall, G.Z., 2007. Hindcast of winds, waves and currents in northern Gulf of Mexico in Hurricanes Katrina (2005) and Rita (2005). *Proceedings of Offshore Technology Conference* (Houston, Texas), pp. 638–649.

Chaichitehrani, N., 2012. Investigation of Colored Dissolved Organic Matter and Dissolved Organic Carbon Using Combination of Ocean Color Data and Numerical Model in the Northern Gulf of Mexico. Baton Rouge, Louisiana: Louisiana State University, Master's thesis, 112p.

Chaichitehrani. N.; D'Sa, E.J.; Ko, D.S.; Walker, N.D.; Osburn, C.L., and Chen, R.F., 2014. Colored dissolved organic matter dynamics in the northern Gulf of Mexico from ocean color and numerical model results. *Journal of Coastal Research,* 30(4), 800–814.

Chen, C.; Beardsley, R.C., and Cowles, G., 2006. *An Unstructured Grid, Finite-Volume Coastal Ocean Model, FVCOM User Manual*. Dartmouth, Massachusetts: University of Massachusetts Dartmouth, 324p.

Chen, Q.; Wang, L.X., and Tawes, R., 2008. Hydrodynamic response of northeastern Gulf of Mexico to hurricanes. *Estuaries and Coasts,* 31(6), 1098–1116.

Chen, Q.; Wang, L.X., and Zhao, H.H., 2009. Hydrodynamic investigation of coastal bridge collapse during Hurricane Katrina. *Journal of Hydraulic Engineering,* 135(3), 175–186.

Church, J.A.; Joyce, T.M, and Price, J.F., 1989. Current and density observations across the wake of Hurricane Gay. *Journal of Physical Oceanography,* 19(2), 259–265.

Cooper, C. and Thompson, J.D., 1989a. Hurricane-generated currents on the outer continental shelf. 1. Model formulation and verification. *Journal of Geophysical Research—Oceans,* 94(C9), 12513–12539.

Cooper, C. and Thompson, J.D., 1989b. Hurricane-generated currents on the outer continental shelf. 2. Model sensitivity studies. *Journal of Geophysical Research—Oceans,* 94(C9), 12540–12554.

Csanady, G.T., 1972. Response of large stratified lakes to wind. *Journal of Physical Oceanography,* 2(1), 3–13.

DHI, 2015. *Mike 21 Toolbox, User Manual*. Horsholm, Denmark: Danish Hydraulic Institute.

Dietrich, J.C.; Zijilema, M.; Westrink, J.J.; Holthuijsen, L.H.; Dawson, C.; Luettich, R.A.; Jensen, R.E.; Smith, J.M.; Stelling, G.S., and Stone, G.W., 2011. Modeling hurricane waves and storm surge using integrally-coupled, scalable computations. *Coastal Engineering,* 58(1), 45–65.

Elsberry, R.L.; Fraim, T.S., and Trapnell, R.N., 1976. A mixed layer model of oceanic thermal response to hurricanes. *Journal of Geophysical Research,* 81(6), 1153–1162.

Keen, T.R. and Glenn, S.M., 1998. Factors influencing model skill for hindcasting shallow water currents during Hurricane Andrew. *Journal of Atmospheric and Oceanic Technology,* 15(1), 221–236.

Keen, T.R. and Glenn, S.M., 1999. Shallow water currents during Hurricane Andrew. *Journal of Geophysical Research—Oceans,* 104(C10), 23443–23458.

Knabb, R.D.; Rhome, J.R., and Brown, D.P., 2005. *Tropical Cyclone Report: Hurricane Katrina*. http://www.nhc.noaa.gov/data/tcr/AL122005_Katrina.pdf.

Large, W.G. and Pond, S., 1981. Open ocean momentum flux measurements in moderate to strong winds. *Journal of Physical Oceanography,* 11(3), 324–336.

Ly, L.N., 1994. A numerical study of sea level and current responses to Hurricane Frederic using a coastal ocean model for the Gulf of Mexico. *Journal of Oceanography,* 50(6), 599–616.

Lyons, R.; Panofsky, H.A., and Wollaston, S., 1964. The critical Richardson number and its implication for forecast problems. *Journal of Applied Meteorology,* 3(2), 136–142.

Makin, V.K., 2003. A note on a parameterization of the sea drag. *Boundary-Layer Meteorology,* 106(3), 593–600.

Makin, V.K., 2005. A note on the drag of the sea surface at hurricane winds. *Boundary-Layer Meteorology,* 115(1), 169–176.

Miner, M.D.; Kulp, M.A.; FitzGerald, D.M., and Georgiou, I.Y., 2009. Hurricane associated ebb-tidal delta sediment dynamics. *Geology,* 37(9), 851–854.

Mitchell, D.A.; Teague, W.J.; Jaroz, E., and Wang, D.W., 2005. Observed currents over the outer continental shelf during Hurricane Ivan. *Geophysical Research Letters,* 32(11). doi:10.1029/2005GL023014

NOAA (National Oceanic and Atmospheric Administration), 2016. *NOAA Gulf of Mexico Data Atlas*. https://gulfatlas.noaa.gov/catalog/.

Pan, J. and Sun, Y., 2013. Estimate of ocean mixed layer deepening after a typhoon passage over the South China Sea by using satellite data. *Journal of Physical Oceanography,* 43(3), 498–506.

Pedlosky, J., 1979. *Geophysical Fluid Dynamics*. New York: Springer, 710p.

Powell, M.; Houston, S.; Amat, L., and Morrisseau-Leroy, N., 1998. The HRD real-time hurricane wind analysis system. *Journal of Wind Engineering and Industrial Aerodynamics,* 77–78, 53–64.

Powell, M.; Houston, S., and Reinhold, T., 1996. Hurricane Andrew's landfall in South Florida.Part I: Standardizing measurements for documentation of surface wind fields. *Weather Forecasting,* 11(3), 304–328.

Price, J.F.; Sanford, T.B., and Forristall, G.Z., 1994. Forced stage response to a moving hurricane. *Journal of Physical Oceanography*, 24(2), 233–260.

Rego, J.L. and Li, C., 2009. On the receding of storm surge along Louisiana's low-lying coast. *In:* da Silva, C.P. (ed.), *Proceedings from the International Coastal Symposium (ICS) 2009, Volume II* (Lisbon, Portugal). *Journal of Coastal Research*, Special Issue No. 56, pp. 1045–1049.

Rego, J.L. and Li, C., 2010. Storm surge propagation in Galveston Bay during Hurricane Ike. *Journal of Marine Systems,* 82(4), 265–279.

Reynolds, R.W. and Smith, T.M., 1994. Improved global sea surface temperature analyses using optimum interpolation. *Journal of Climate,* 7(6), 929–948.

Sanford, T.B.; Black, P.G.; Haustein, J.R.; Feeney, J.W.; Forristall, G.Z., and Price, J.F., 1987. Ocean response to a hurricane. Part I: Observations. *Journal of Physical Oceanography,* 17(11), 2065–2083.

Shen, B.W.; Atlas, R.; Reale, O.; Lin, S.J.; Chen, J.D.; Chang, J.; Henz, C., and Li, J.L., 2006. Hurricane forecasts with a global mesoscale resolving model: Preliminary results with Hurricane Katrina (2005). *Geophysical Research Letters,* 33(13), L13813.

Siadatmousavi, S.M.; Allahdadi, M.N.; Chen, Q.; Jose, F., and Roberts, H.H., 2012. Simulation of wave damping during a cold front over the muddy Atchafalaya shelf. *Continental Shelf Research,* 47, 165–177.

Stewart, R.H., 2009. *Introduction to Physical Oceanography*. College Station, Texas: Texas A&M University, 345p.

Stone, G.W.; Jose, F.; Luo, Y.; Siadatmousavi, S.M., and Gibson, W.J., 2009. A WAVCIS-based ocean observing station off Eglin Air Force Base, Fort Walton, Florida. *Proceeding of OCEANS 2009* (Biloxi, Mississippi, MTS/IEEE), pp. 1–9.

Teague, W.J.; Jarosz, E.; Wang, W.D., and Mitchell, D.A., 2007. Observed oceanic response over the upper continental slope and outer shelf during Hurricane Ivan. *Journal of Physical Oceanography,* 37(9), 2181–2206.

Tehrani, N.C.; D'Sa, E.J.; Osburn, C.L.; Bianchi, T.S., and Schaeffer, B.A., 2013. Chromophoric dissolved organic matter and dissolved organic carbon from sea-viewing wide field-of-view sensor (SeaWiFS), moderate resolution imaging spectroradiometer (MODIS) and MERIS sensors: Case study for the northern Gulf of Mexico. *Remote Sensing,* 5(3), 1439–1464.

Wang, D.P. and Oey, L.Y., 2008. Hindcast of waves and currents in Hurricane Katrina. *Bulletin of the American Meteorological Society,* 89(4), 487–495.

Willmott, C.J., 1981. On the validation of models. *Physical Geography,* 2(2), 184–194.

Wiseman, W.J.; Rabalais, N.N.; Turner, R.E.; Dinnel, S.P., and Macnaughton, A. 1997. Seasonal and interannual variability within the Louisiana coastal current: Stratification and hypoxia. *Journal of Marine Systems,* 12, 237–248.

Xu, K.H.; Mickey, R.C.; Chen, Q.J.; Harris, C.K.; Hetland, D.; Hu, K., and Wang, J., 2016. Shelf sediment transport during Hurricanes Katrina and Rita. *Computers and Geosciences,* 90B(May 2016), 24–39. doi:10.1016/j.cageo.2015.10.009

Zhang, J.L. and Steele, M., 2007. Effect of vertical mixing on the Atlantic water layer circulation in the Arctic Ocean. *Journal of Geophysical Research—Oceans,* 112(C4). doi:10.1029/2006JC003732